iJRASET
International Journal For Research in
Applied Science and Engineering Technology

INTERNATIONAL JOURNAL FOR RESEARCH

IN APPLIED SCIENCE & ENGINEERING TECHNOLOGY

Volume: 5 **Issue:** XI **Month of publication:** November 2017

DOI:

Enhancing of DFIG During Three-Phase Fault Using Parallel Interleaved Converters and Dynamic Resistor

V. Srinivasulu[1], N. Dharani Kumar[2]
[1]Communication & Signal processing M. Tech, [2]Assistant Professor in ECE Department
R. V. R& J. C College of Engineering, Guntur, Andhra Pradesh (522019), India

Abstract-This study presents a new control scheme for DFIG wind turbine having Parallel interleaved converters (PIC) configuration and series dynamic braking resistor (SDBR) connected to it. The converters in the configuration would help to increase current capability. While SDBR helps in post fault recovery. Combined effect of these two was implemented in power system computer aided design and electromagnetic transient including DC simulation environment for a severe three phase to ground fault. The study approach was compared with conventional DC chopper and Crowbar rotor circuit protection for DFIG. The space vector modulation of the PIC result in maximum value of change in common mode voltage, leads to better switched output results of the voltage source converter leg so we get better performance of wind turbine variables using the scheme of PIC and SDBR.
***Keywords: Double Fed Induction Generator(DFIG),* Parallel Interl eaved Converter(PIC), Series Dynamic Breaking Resistor(SDBR).**

I. INTRODCUTION

There are many ways types of faults in power systems, when we consider three phase faults are the severe ones at the point of common coupling. Fixed speed technology wind generators that possesses good characteristics like brushless and rugged construction, low cost and simple operations are used earlier. During fault conditions these require FACTS devices for stability which are expencive. Several FACTS devices have been used to enhance the stability of the fixed speed wind turbines in the literature [1–4]. The recent grid requirements demand that wind turbines should have a good performance with respect to voltage control capability and robust behaviour against frequency and voltage variations under fault conditions. The amount of necessary dynamic reactive power compensation depends generally on the type of wind turbine generator system and is influenced by relevant electrical and mechanical parameters of that system. Two sets of variable speed wind turbine are used to provide dynamic reactive power to the grid system; the doubly fed induction generator (DFIG) and the permanent magnet synchronous generator. The former possesses lower power converter rating, hence widely in use. This is typically 20–30%, and therefore its size, cost, and losses are much smaller compared with a full size power converter used in the later variable speed wind generator technology [5]. Besides, it has frequency converters that can operate at high sampling and switching frequencies [9] in its pulse width modulation (PWM), making it superior for independent control of active and reactive power during grid disturbances [10]. Moreover, the dynamic slip control and pitch control are the other important characteristics which help to enhance the system stability of this wind turbine technology. Many techniques have been presented to improve the stability of the DFIG, approach of protection schemes for DFIG using crowbar system and the DC-chopper system was investigated in [15], while a comparative study for both schemes were reported in [16]. Augmentation of DFIG wind turbine with Static Series Compensator (SSC), a Dynamic Voltage Restorer (DVR) and STATCOM were reported in [17–20], in which considerable
improvement of the stability performance of the DFIG system during grid disturbances was achieved. The use of a series dynamic braking resistor (SDBR) to boost the stability of large wind farms was presented in [21]. A further investigation of connecting SDBR switch to the rotor side converter (RSC) of the DFIG and the stator side were presented in [22, 23] respectively. Passive and connections involving series antiparallel thyristors [26] to the stator side of a variable speed DFIG system, already exist in the literature. A proposed current controlled voltage source converter (VSC) instead of voltage control VSC was presented in [27–29]. Since the DFIG wind turbine power converters are vulnerable and fragile during transient conditions, it is imperative to protect and keep the wind turbine in operation to avoid damages. A salient requirement for the DFIG is to inject its three phase rotor circuit with a controllable frequency and magnitude voltage. The AC three phase voltage can be controlled using various switching techniques

ranging from six step switching [30], PWM [31], and space PWM [32]. The conventional DFIG system uses two level back to back power converters, which is hardly used for high power applications. Consequently, a multilevel converter using PWM are highly preferred for wind power generation application [33, 34].The main reason behind this is that the multilevel power converter structure for wind turbines increases the power rating as well as reduces the stress on the insulated-gate bipolar transistors (IGBTs) switches and therefore enhances the voltage waveforms, in addition to reducing the harmonic content. In [35–38], it was established that the harmonic quality of the resultant voltage waveforms in high power applications could be improved by interleaving the carrier signals of the parallel connected VSCs. In [39, 40], the reliability analysis and robustnessof MW level IGBT module under short circuit events were carried out, respectively. Power quality improvement for DFIG system

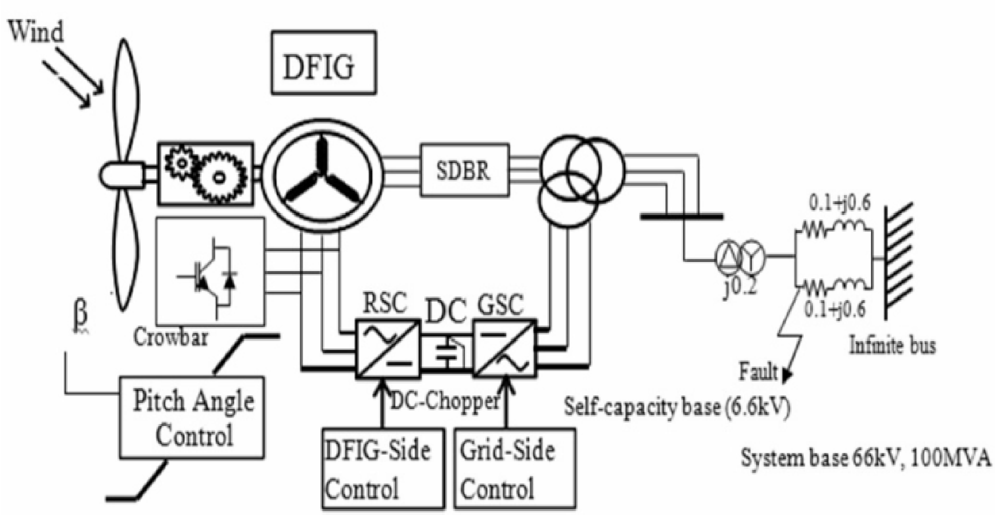

Figure1: Model System with conventional protection schemes

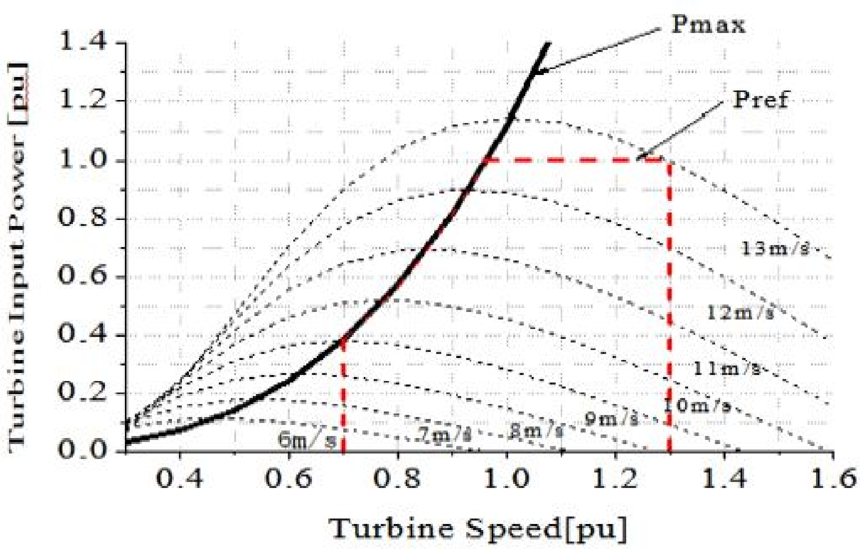

Figure2: Turbine characteristics with MPPT

using different types of rotor converters was presented in [41], where it was reported that higher harmonic contents occur with the six-step 2 level IGBT inverter due to low switching frequency, thus the performance of this type of inverter system is reduced.

ISSN: 2321-9653; IC Value: 45.98; SJ Impact Factor:6.887
Volume 5 Issue XI November 2017- Available at www.ijraset.com

Generator type	(DFIG)
Rated voltage	690 V
Stator resistance	0.01 pu
Stator leakage reactance	0.15 pu
Magnetizing reactance	3.5 pu
Rotot resistance	0.01 pu
Rotor leakage reactance	0.15 pu
Inertia constant	1.5 s
Rated voltage	690 V
Stator resistance	0.01 pu
Stator leakage reactance	0.15 pu

Table 1: Generator Parameters

Parameters	Ratings
DC-link voltage	1.5 kv
DC-link capacitor	50,000 µF
Device for power converter	IGBT
PWM carrier frequency	2 kHz
Upper limit of DC voltage	1.65 kV(110%)
Lower limit of DC voltage	0.75 kV(50%)
Internal resistance	0.2 Ω

Table2: Rating and parameters of excitation circuit

II. ANTENNA DESIGN

A. Wind Generation Model and Convection Protection Scheme

The DFIG wind turbine is subjected to a three-phase to ground fault at point F. An aggregated wind turbine capacity of 50 MVA was used in this study with a system base of 100 MVA. The parameters of the wind turbine are given in Table 1 [14]. Basically the primary components required in the modelling of a wind turbine system are the turbine rotor or prime mover, a shaft and a gearbox unit. The aerodynamic torque and the mechanical power of a wind turbine are given by [14]: where ρ is the air density, R is the radius of the turbine, Vw is the wind speed, Cp(λ, β) is the power coefficient. The excitation parameters of the wind turbine are given in Table 2. The rated wind speed of the wind turbine is 12.43 m/s and it occurs at 0.96 pu turbine speed (Fig. 2). The range of operation of the wind turbine speed is 0.7 pu (minimum) to 1.3 pu (maximum) as displayed by the red line in Fig. 2. A rated wind speed value of 12.4 m/s in (3) gives the optimum speed of the wind turbine. In section A of Fig. 3, the threshold value of the wind speed is 11 m/s for controlling high and low wind speed periods via a comparator system. The control function is used to generate the reference power of the wind turbine. If the wind speed is above 11 m/s, in the case of its rated value of 12.43 m/s, from (1), the reference power (Pref1) becomes 1 pu (at 0.96 pu wind turbine speed). Moreover, if the wind speed is below 11 m/s, for example 9 m/s, then from (2), the reference power (Pref2) becomes 0.4 pu (at 0.7 pu turbine minimum speed).

$$T_M = 0.5\rho C_t(\lambda)\pi R^3 V_w^2 \text{ [NM]}$$

$$P_{wt} = 0.5\rho C_p(\lambda,\beta)\pi R^2 V_w^3 \text{ [W]}$$

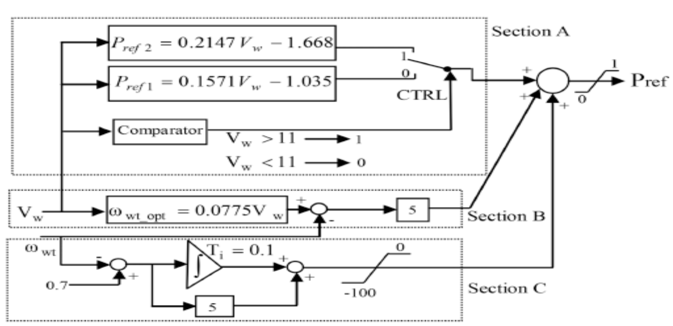

Figure3: control block to determine active power reference p_{ref}

International Journal for Research in Applied Science & Engineering Technology (IJRASET)
ISSN: 2321-9653; IC Value: 45.98; SJ Impact Factor:6.887
Volume 5 Issue XI November 2017- Available at www.ijraset.com

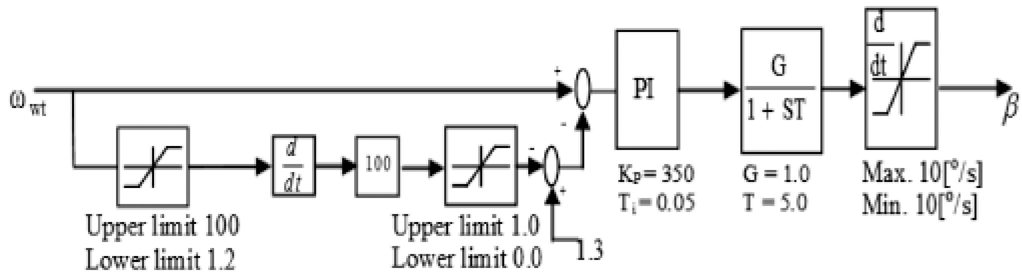

Figure 4: Pitch controller for DFIG wind tirbine

$$P_{\text{ref}_1} = 0.1571 V_w - 1.035 \quad [\text{pu}]$$

$$P_{\text{ref}_2} = 0.2147 V_w - 1.668 \quad [\text{pu}]$$

III. PROPESED MODEL SCHEME OF STUDY

The control strategies of the DC chopper and the crowbar are already in the literature. Details of the SDBR control strategy will be presented in the subsequent section. voltage to ± *V*dc, whereas for the clamped discontinuous PWM schemes, this value is ±(2*V*dc/3). The flux in the common leg can be reduced by reducing the time integral of the change in the CM voltage. This is achieved by avoiding the use of zero voltage vectors. This work employs the near state PWM scheme that has three nearest active voltage vectors to synthesise the reference voltage vector ***V***ref. The switching table sequence in Fig. 6 is based
on the sequence of numbers in which the corresponding voltage vectors are applied considering the space vector diagram in Fig. 7 which is divided into six regions. The switching sequence 612 is used in both sub-sector 1 where $0° \leq \phi \leq 30°$ and sub-sector 12 where $330° \leq \phi \leq 360°$. Theoretically, these two sub-sectors together make up region 1 and the geometrical formation of the reference voltage ***V***ref in this region is shown in Fig. 7. The active voltage vectors ***V***1, ***V***2 and ***V***6 in the switching table are given as

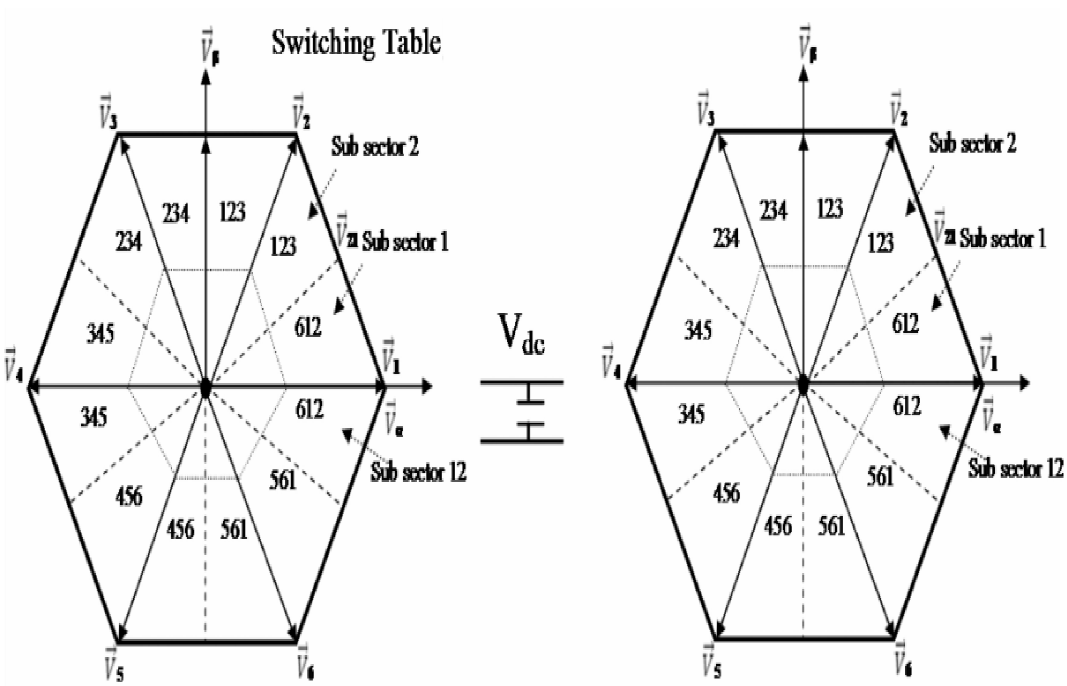

Figure 6: Switching table of PIC

$$T_1 = \left(\sqrt{3}\frac{V_{\alpha,r}}{V_{dc}} + \frac{V_{\beta,r}}{V_{dc}} - 1\right)T_s$$

$$T_2 = \left(1 - \frac{2}{\sqrt{3}}\frac{V_{\alpha,r}}{V_{dc}}\right)T_s$$

$$T_6 = \left(1 - \frac{1}{\sqrt{3}}\frac{V_{\alpha,r}}{V_{dc}} - \frac{V_{\beta,r}}{V_{dc}}\right)T_s$$

where, *T*1, *T*2 and *T*3,, are the respective dwell times of the active voltage vectors, *T*s is the switching time, *Vα*, *Vβ* are the *α*, *β* components represented in Fig. 6 and *Vα*,r and *Vβ*,r are the *α* and *β* components at the start of the region and these are given for region 1 as: vectors, two near opposing active voltage vectors (***V***3, ***V***6) are used. Consequently, the linear operation over the entire modulation range (0 ≤ *M* ≤ 2/ 3) is obtained. In the two level converter system only eight voltage vectors that includes two nulls is generated. The complex switching circuitry of the two level interleaved VSCs system allows much possibility for appropriate voltage vector selection to satisfy the commutation condition.

An SDBR with value 0.01 pu is connected to the stator of the DFIG system. The SDBR control is achieved by inserting the resistor in the stator of the DFIG during a grid fault, thereby increasing its terminal voltage. Consequently, the electrical torque and power of the wind turbine is mitigated. Since the cost of a bypass switch is relatively cheaper than a circuit breaker, the SDBR used in this study, uses a bypass switch that is normally on, but when voltage dip below 0.9 pu occurs due to a grid fault, it opens to allow current pass through the small series resistance. When voltage is recovered above a certain set value of 0.9 pu for the grid voltage, the bypass switch closes and the stator circuit restores to its normal state. The effect of a grid fault on the DFIG rotor current is analysed as follows based on [22]. The voltage expression for phase-a is

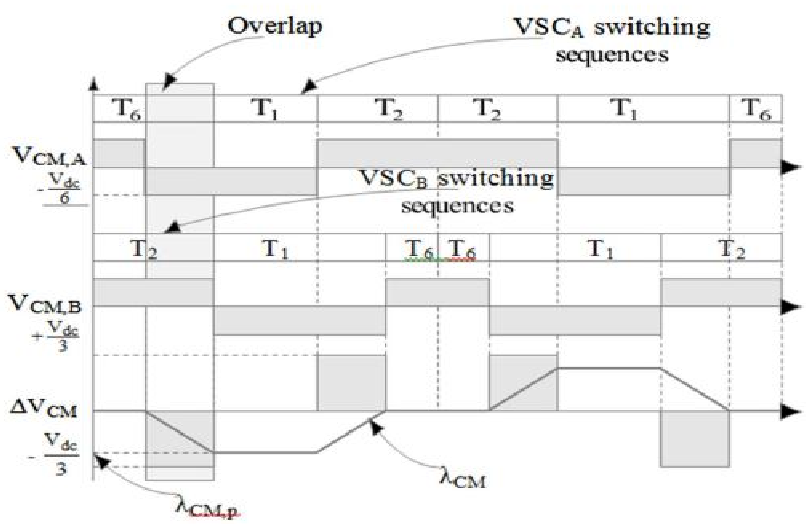

Figure 8: switching sequences and CM voltages for VSCs A and B

$$v_{ra}(t) = \mathrm{Re}[v_{ro}^{r}] + r_{21} \cdot i_{ra}(t) + \sigma L_{21}\frac{\mathrm{d}i_{ra}(t)}{\mathrm{d}t}$$

$$v_{ro}^{r} = \frac{L_{mu}}{L_1}\left(\frac{d}{dt} - j\omega_r\right)\psi_s$$

$$\sigma = 1 - \frac{L_{mu}^2}{L_1 L_{21}}$$

International Journal for Research in Applied Science & Engineering Technology (IJRASET)
ISSN: 2321-9653; IC Value: 45.98; SJ Impact Factor:6.887
Volume 5 Issue XI November 2017- Available at www.ijraset.com

$$v_{ro}^{r} = (1-p)V_s \frac{L_{mu}}{L_1} s\, e^{js\omega_s t} - \frac{L_{mu}}{L_1}\left(\frac{1}{\tau_s} + j\omega_r\right)\frac{pV_s}{j\omega_s} e^{-t/\tau_s}$$

$$\tau_r = \frac{\sigma L_{21}}{r_{21}}, \quad \tau_s = \frac{L_1}{r_1}, \quad \tau = \frac{\tau_r \tau_s}{\tau_s - \tau_r}$$

$$v_{ro}^{r} \simeq V_s \frac{L_{mu}}{L_1}\left[s(1-p)\, e^{js\omega_s t} - (1-s)p\, e^{-(t/\tau_s)}\right]$$

$$i_{ra}(t) = i_{dc} + i_{vr} + i_{vrf} + i_{vrn}$$

$$i_{dc} = \begin{cases} i_{ra}(t_0^-) - \dfrac{1}{\sigma L_{21}}\dfrac{\tau_r}{1+\tau_r^2(s\omega_s)^2}\left[V_r\cos\beta - V_s\dfrac{L_{mu}}{L_1}s(1-p)\right] \\ \qquad \dfrac{1}{\sigma L_{21}}V_s\dfrac{L_{mu}}{L_1}(1-s)p\dfrac{\tau}{1+\tau^2\omega_r^2} \\ e^{-(t/\tau_r)} \end{cases}$$

$$i_{vr} = \frac{V_r}{\sigma L_{21}}\left[\begin{array}{l} \dfrac{\tau_r}{1+\tau_r^2\omega_r^2}\cos(s\omega_s t + \beta) \\ +\dfrac{\tau_r^2\omega_r}{1+\tau_r^2\omega_r^2}\sin(s\omega_s t + \beta) \end{array}\right]$$

$$i_{vrf} = -\frac{1}{\sigma L_{21}}V_s\frac{L_{mu}}{L_1}s(1-p)\left[\begin{array}{l} \dfrac{\tau_r}{1+\tau_r^2(s\omega_s)^2}\cos(s\omega_s t) \\ +\dfrac{\tau_r^2 s\omega_s}{1+\tau_r^2(s\omega_s)^2}\sin(s\omega_s t) \end{array}\right]$$

$$i_{vrn} = \frac{V_s}{\sigma L_{21}}\frac{L_{mu}}{L_1}(1-s)p\left[\frac{\tau}{1+\tau^2\omega_r^2}\cos(\omega_r t) + \frac{\tau^2\omega_r}{1+\tau^2\omega_r^2}\sin(\omega_r t)\right] e^{-(t/\tau_s)}$$

The equations involves voltage and currents produced due to stator flux. σ is the leakage factor, while Lmu, L1, L21, r21, ωr, ψs are the magnetising, stator, and rotor inductances, rotor resistance, angular rotor frequency and stator flux, respectively.

Let output voltage of the converter be V_{ra}. where β is the phase-a rotor voltage angle at the moment the fault occurs, ωs, $s\omega$s, are the synchronous and slip angular frequencies, respectively. Considering a symmetrical voltage disturbance on the stator side Vs, that is, a three phase step amplitude change from Vs to $(1-p)V$s (where p is the voltage dip ratio), can exceed the maximum voltage that the rotor converter can generate,

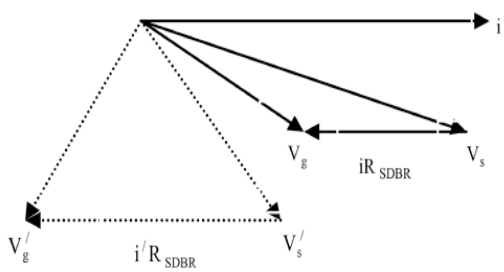

Figure 9: Effect of SDBR stability

International Journal for Research in Applied Science & Engineering Technology (IJRASET)
ISSN: 2321-9653; IC Value: 45.98; SJ Impact Factor:6.887
Volume 5 Issue XI November 2017- Available at www.ijraset.com

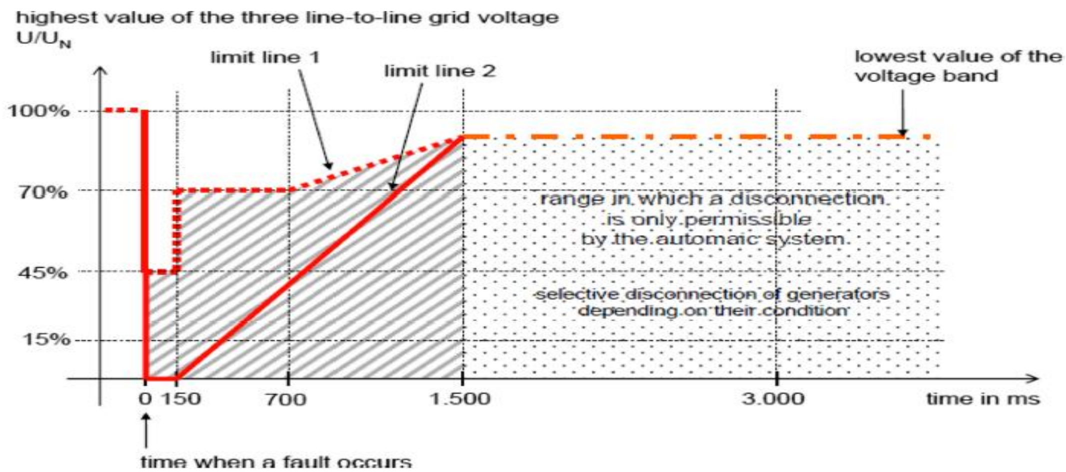

Figure 10: Fault ride through requirement for wind farm

IV. GRIDE CODES

The most worrying problem for wind farms is a voltage dip in the grid during a grid fault. The magnitude of the voltage can be controlled by the reactive power exchange. Fig. 10 displays the typical requirement for fault-ride through grid code. The wind farm must remain connected to the grid if the voltage drop is within the defined r.m.s. value and its duration is also within the defined period as shown in the curve [43].

V. SIMULATION RESULTS AND DISCUSSIONS

Simulations were run for two scenarios. The first scenario considers the conventional protection scheme for the wind turbine and the proposed PIC scheme. In the second scenario, the coordinated control of the use of the SDBR and PIC in enhancing the DFIG wind turbine was analysed.

Scenario 1: Conventional protection schemes and the proposed scheme for DFIG

The model system in Fig. 1 was subjected a severe three-phase to ground fault and responses of the DC-link voltage of the wind turbine was observed using the conventional DC-chopper and crowbar schemes. These responses where further compared with that obtained using the proposed parallel interleaved converter scheme. On basis of the response in Fig. 11*a*, the DC chopper gave a better performance than the expensive crowbar system as reported in the literature because of faster settling time with less oscillations. Hence, the DC chopper would be used for further analysis in this work. When the converters were interleaved based on the switching table in Fig. 6 and the formation of the reference space vector, more current would be in circulation because of the active voltage vectors and their dwell times as described by the equations in Section 3 for the PIC system. A further investigation of interleaving only the RSC or only the GSC was compared with when both sides of the converters were interleaved as shown Fig. 11*b*. Interleaving both converters of the wind turbine creates room for more switching commutation of the IGBTs with increased circulating current and more reactive power provision. Thus the power converters are more protected during transient conditions.

Scenario 2: Enhancing the DFIG wind turbine using the proposed scheme and SDBR

A scenario whereby an SDBR connected to the stator of the DFIG variable speed wind turbine as shown in the model system was further investigated in conjunction with the PIC. Some of the Responses. The coordinated control of the PIC and SDBR topology improves the performance of DFIG wind turbine because the induced overvoltage caused during transient periods is limited by controlling the rotor overvoltage and same time limits the high rotor current of the wind turbine as described by (14)–(32). Consequently, the rotor current limitation reduces the charging current to the DC-link capacitor, hence avoiding DC-link overvoltage/under voltage which could damage the DFIG power converter. The SBDR can also balance the active power of the

ISSN: 2321-9653; IC Value: 45.98; SJ Impact Factor:6.887
Volume 5 Issue XI November 2017- Available at www.ijraset.com

DFIG based on the displaced dynamic power shown in the model system and thus, improves the DFIG wind generator stability during grid fault. Furthermore, the SDBR increases the wind generator output which therefore reduces its speed increase during transient periods considering the phasor diagram. The combination of all these effects improves the terminal voltage and entire performance of the DFIG system using the proposed scheme. The terminal voltage of the DFIG system follows the grid requirement during transient as it was able to recover within the stipulated time to avoid the shutdown of the wind farm. However, the scenario where the SDBR was implemented gave a fast recovery of the wind turbine terminal voltage. A better performance of the wind turbine terminal voltage was achieved with the coordinated control of the SDBR and PIC proposed strategy.

VI. SIMULATION RESULTS

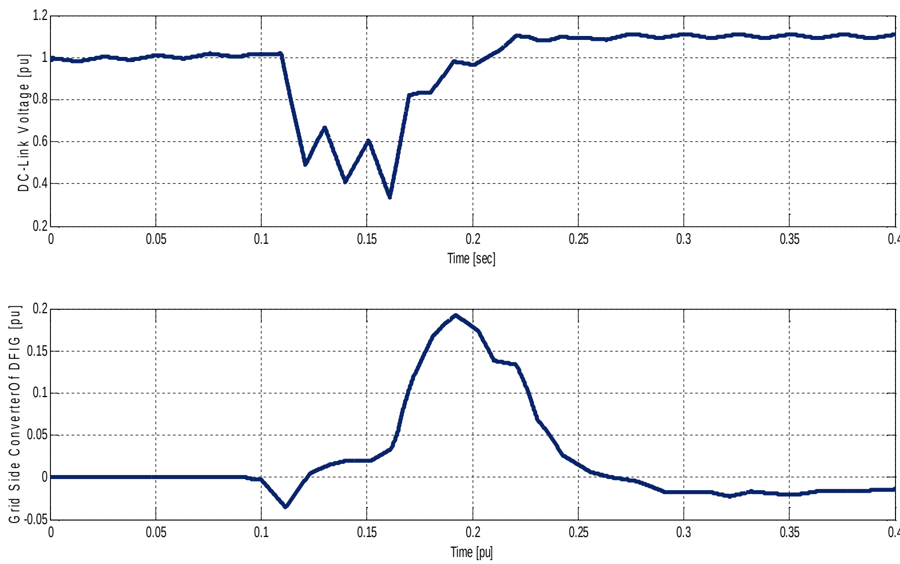

Figure 11: Results of simulation dc link voltage for parallel inter leaved converter(PIC), Grid side voltage for PIC both converters and Terminal voltage of DFIG with SDBR and PIC.

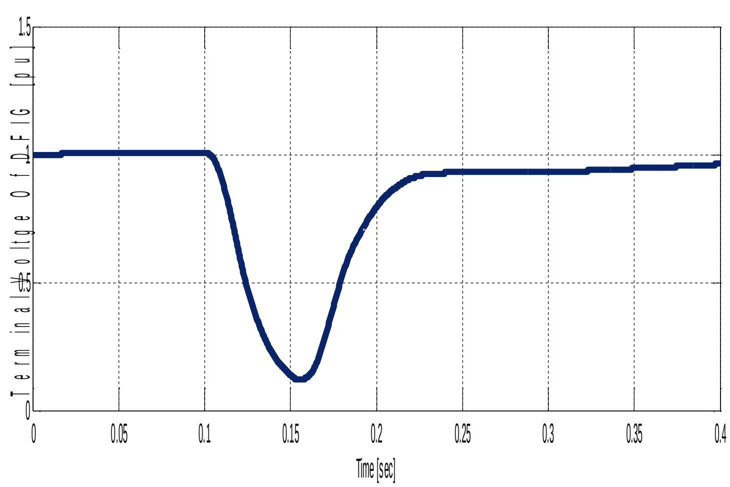

Figure 12: Results of terminal voltage

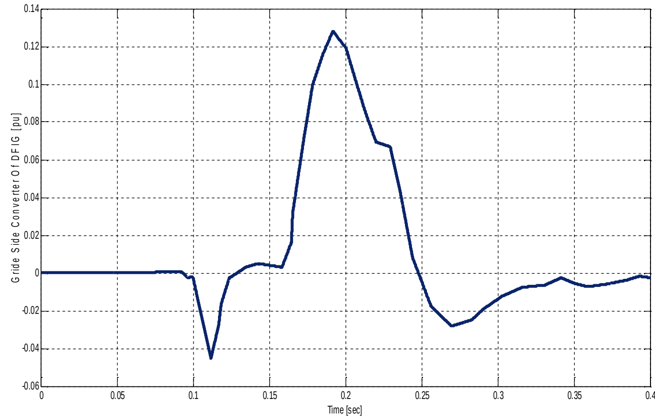

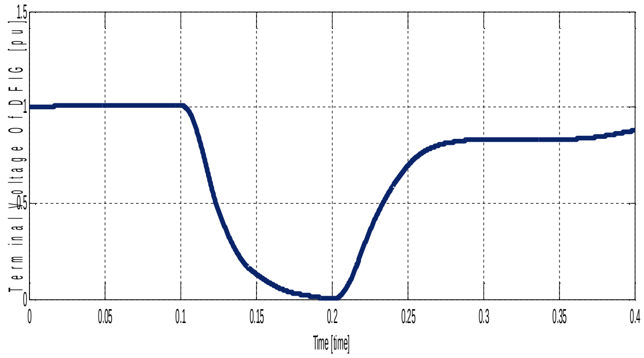

Figure 13shows The grid side converter voltage with SDBR and secod one is for PIC on rotor side converter

VII. CONCLUSION

The performance of Doubly Fed Induction Generator (DFIG) variable speed wind turbine with parallel interleaved VSCs and a dynamic resistor was investigated during a grid fault. Interleaving the carrier signals in parallel configuration of the VSC system in a variable speed wind turbine can improve its performance during transient conditions. This is because, it allows for much more possibilities of appropriate voltage vector selection to enhance switching and commutation condition. To further enhance the performance of the DFIG wind turbine, a coordinated control of the parallel interleaved converter and a SDBR of low value were suggested. The performance of the wind turbine was analysed considering a severe three-phase to ground fault to test the rigidity of the wind turbine system. The simulation results presented show improved performance of the variable speed wind turbine system using the proposed scheme.

REFERENCES

[1] El-Sattar, A.A, Saad, N. H., Shams, El-Dein M.Z.: 'Dynamic response of doubly fed induction generator variable speed wind turbine under fault', Electr. Power Syst. Res., 2008, 78, 7 pp. 1240–1246

[2] Chowdhury, B.H., Chellapilia, S.: 'Doubly-fed induction generator control for variable speed wind power generation', Electr. Power Syst. Res., 2006, 76, pp. 786–800

[3] Yao, J., Li, H., Liao, Y., et al.: 'An improved control strategy of limiting the DC-link voltage fluctuation for a doubly fed induction wind generator', IEEE Trans. Power Electron., 2008, 23, (3), pp. 1205–1213

[4] Rodriguez, M., Abad, G., Sarasola, I., et al.: 'Crowbar control algorithms for doubly fed induction generator during voltage dips'. Presented at the 11th Eur. Conf. Power Electronics Application, Dresden, Germany, September 2005, pp. 1–10

[5] Causebrook, A., Atkinson, D.J., Jack, A.G.: 'Fault ride through of large wind farms using series dynamic braking resistors', *IEEE Trans. Power Syst., 2007,* 22, (3), pp. 966–975

[6] Yang, J., Fletcher, E., O'Reilly, J.: ‘A series dynamic resistor based converter protection schemes for doubly fed induction generator during various fault conditions’, IEEE Trans. Energy Convers., 2010, 25, (2), pp. 422–432
[7] Okedu, K.E., Muyeen, S.M., Takahashi, R., et al.: ‘Comparative study on current and voltage controlled voltage source converter based variable speed wind generator’. Proc. of Int. Conf. on Electric Power and Energy Conversion Systems, Sharjah, UAE, 15-1 November 2011, pp. 1–7
[8] Murphy, J., Turnbull, F.: ‘Power electronics control of AC motors’ (Pergamon, New York, 1988)
[9] Muller, S., Deicke, M., Doncker, R.W.D.: ‘Doubly fed induction generator systems for wind turbine’, IEEE Ind. Appl. Mag., 2002, 8, (3), pp. 26–33
[10] Nabae, A., Takahashi, I., Akagi, H.: ‘A new neutral point clamped PWM inverter’, *IEEE Trans. Ind. Appl., 1981*, 17, pp. 518–523
[11] Gohil, G., Bede, L., Teodorescu, R., et al.: ‘An integrated inductor for parallel interleaved VSCs and PWM schemes for flux minimization’, IEEE Trans. Ind. Electron., 2015, 62, (12), pp. 7534–7546
[12] Ueda, F., Matsui, K., Asao, M., *et al.:* ‘Parallel connections of pulse width modulated inverters using current sharing reactors’, IEEE Trans. Power Electron., 1995, 10, (6), pp. 673–679
[13] Nashed, M.N., Eskander, M.N.: ‘Comparing the quality of power generated from DFIG with different types of rotor converters’, J. Electromagn. Anal. Appl., 2012, 4, pp. 21–29
[14] E.ON NETZ GmbH: ‘Grid connection regulation for high and extra high voltage’. 2006
[15] Erlich, I., Wrede, H., Feltes, C.: ‘Dynamic behavior of DFIG-based wind turbine during grid faults’, IEEJ Trans. Ind. Appl., 2008, 128, (4), p. 396
[16] Karim-Davijani, H., Sheikjoleslami, A., Livani, H., et al.: ‘Fuzzy logiccontrol of doubly fed induction generator wind turbine’, World Appl. Sci. J.,2009, 6, (4), pp. 499–508
[17] Yang, J., Fletcher, E., O'Reilly, J.: ‘A series dynamic resistor based converter protection schemes for doubly fed induction generator during various fault conditions’, IEEE Trans. Energy Convers., 2010, 25, (2), pp. 422–432

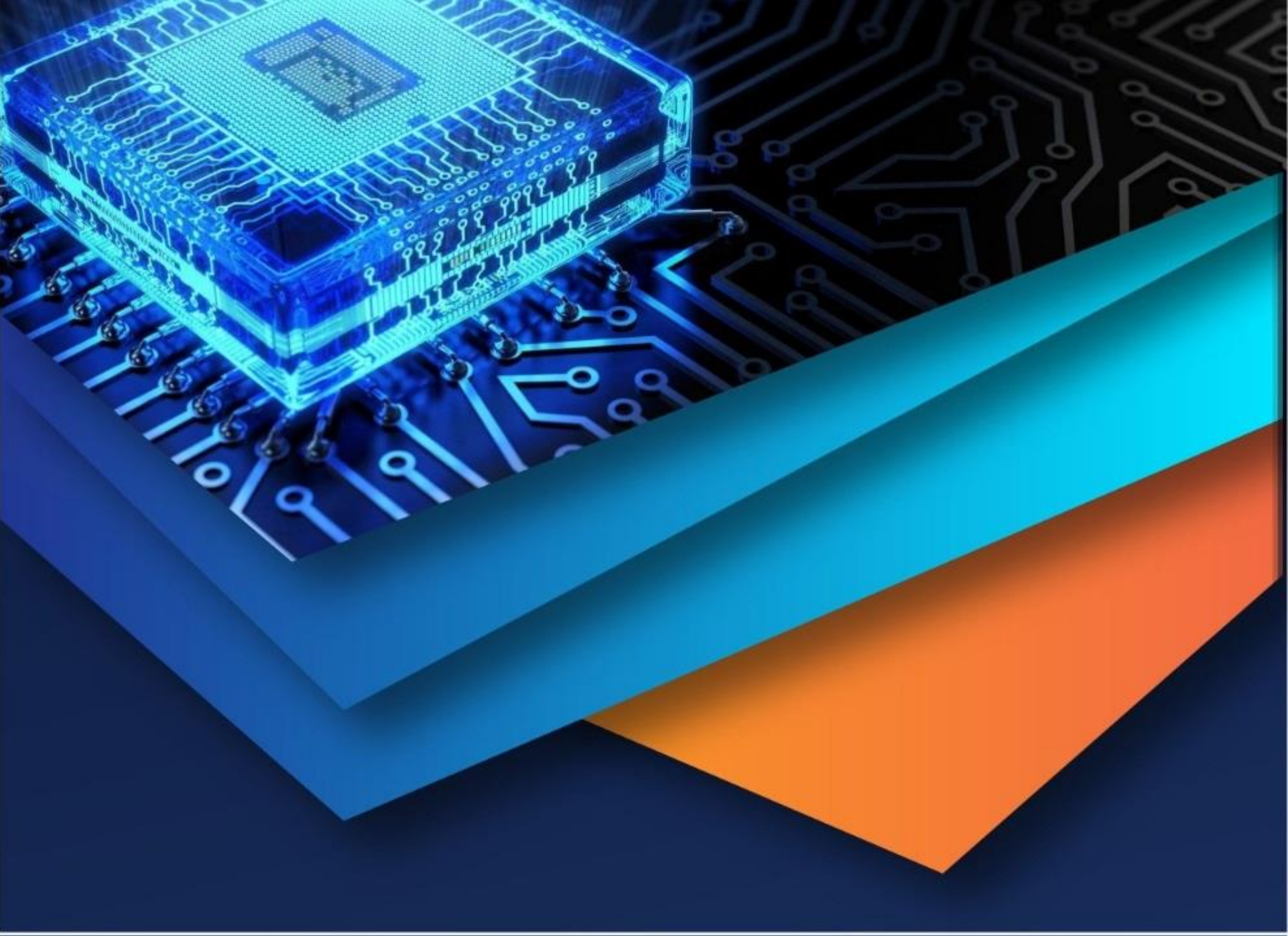

10.22214/IJRASET

INDEX COPERNICUS 45.98

ISRA JIF IMPACT FACTOR: 7.129

TOGETHER WE REACH THE GOAL IMPACT FACTOR: 7.429

INTERNATIONAL JOURNAL FOR RESEARCH

IN APPLIED SCIENCE & ENGINEERING TECHNOLOGY